

# Rings Upon Rings: A New Approach to Pattern Recognition in Ring-Imaging Čerenkov Detectors

Roy F. Schwitters\*  
*Department of Physics*  
*University of Texas at Austin*

May, 1998

## 1 Introduction

Ring-imaging Čerenkov detectors (RICH) are a well developed technique<sup>1</sup> for identifying high-speed charged particles. In a typical application, the number of Čerenkov photons detected and their characteristic angular distribution are exploited to determine the particle's speed  $v = \beta c$ . This information is usually combined with momentum measurements to estimate the particle's mass and, hence, its identity. RICH detectors use spherical mirrors or other optics to focus Čerenkov photons emitted from charged tracks at a given direction in space to a point on the detector. Photons from a particular track form a circular pattern on the image plane. The centers of these rings are related to the direction of charged tracks; the radius and number of photons detected depend on  $\beta$  of the track.

In many experiments, physics objectives motivate searching for heavier, relatively rare particles against backgrounds of lighter particles of a given momentum range (such as "tagging" kaons amongst pions). The pattern-recognition/data-analysis strategy in these cases involves demonstrating a relative *lack* of photons detected in rings surrounding the charged track, that would be characteristic of the heavier, lower- $\beta$  particle being sought.

In situations where one is interested in highly relativistic particles,  $\beta \sim 1$ , Čerenkov detectors offer attractive possibilities for charged-particle *tracking*, in addition to their traditional roles in particle-identification. Fundamentally, a RICH detector measures the directions of detected photons. By finding rings in the patterns of detected photons, the parent track *direction* can be inferred from knowledge of the ring center. When combined with precise vertex tracking and an analyzing magnet, for example, a RICH

---

\*Work supported in part by US DOE

<sup>1</sup>See, for example, reference [1].

tracker could allow measurements of momenta of relativistic particles with little or no other post-magnet tracking information by comparing track directions before (vertex tracking) and after (RICH) the magnet. (Matching track segments from a vertex tracker and a RICH could be accomplished in the non-bend plane with relatively few or no traditional tracking chambers.)

RICH detectors are capable of providing relatively “non-invasive” measurements of charged tracks over significant regions of solid angle because only the radiator medium and some optics need be placed in the paths of the particles; photon detectors can be moved out of the way with appropriate optical designs, thus potentially reducing the material, both active and inactive, that must be traversed by particles. Some of the factors that could make RICH detectors attractive as tracking systems include:

- RICH detectors are capable of determining track directions to better than a fraction of a milli-radian given reasonably large numbers of detected photons (detecting more than 20 photo-electrons per  $\beta \approx 1$  track is a realistic goal in modern RICH detectors), a well-designed optical system, and moderate dispersion in the radiating medium. This resolution is comparable to typical multi-wire drift chamber systems operating at atmospheric pressure.
- A RICH tracker is insensitive to highly ionizing, relatively slowly moving nuclear fragments.
- In high-rate environments where wire-chamber aging is a consideration, the non-invasive nature of Čerenkov detection and “pixel” organization commonly employed in photon detectors may provide distinct advantages over drift chambers constructed with long anode wires.
- In large, multi-particle spectrometers that must employ RICH detectors for particle identification, overall system cost and complexity may be reduced if the RICH also provides some charged-particle tracking information.

To realize the potential of RICH detectors in charged particle tracking applications, it is desirable to find new pattern-recognition algorithms for event triggering and reconstruction that efficiently find Čerenkov rings and their centers *without* auxiliary tracking information. We suggest here one possible algorithm for doing this.

## 2 Dual-Ring Algorithm

Consider a RICH where the optical system can be characterized by a focal length  $f$ . Photons radiated from a charged track at a Čerenkov angle  $\theta_C$

form a circle of radius  $R = f\theta_C$  at the detector.<sup>2</sup> The *locus* of possible track directions—Čerenkov ring centers—that *could have* generated one of the photons on the Čerenkov ring is also a circle of radius  $R$ , but one centered on the position of the detected photon.

We next imagine superimposing circles of radius  $R$  centered on *every* detected photon as shown schematically in Figure 1. The circles cross at various points inside a radius  $2R$  from the true track center, but *all circles intersect or nearly intersect at the actual track center*, creating a high density of lines or pixels describing them at this *one* point. We propose an algorithm to generate and detect such singularities as a way to recognize Čerenkov rings and to determine their centers. This algorithm relies on information from detected photon information alone.

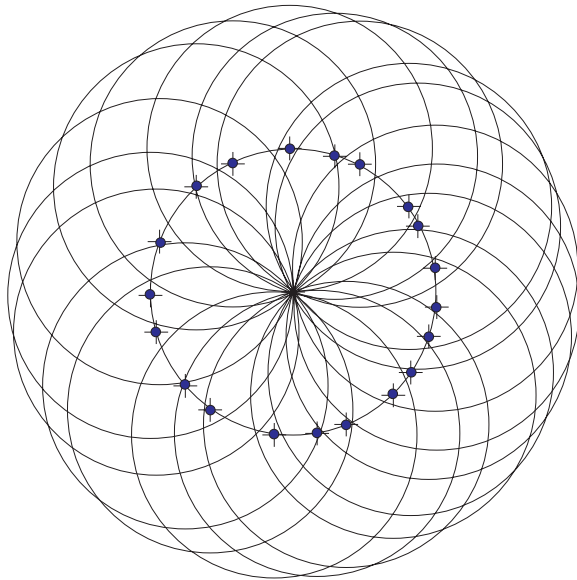


Figure 1: Idealized representation of circles of radius  $R = f\theta_C$  centered on each of a set of Čerenkov photon hits from a single track.

We call the circles centered on each detected photon the “dual representation” of the Čerenkov photon “hit.” The space on which they are superimposed is called the “dual space.” There are dual representations for every possible Čerenkov radius (or value of  $\beta$  above Čerenkov threshold). However, the existence of the limiting value  $\beta \rightarrow 1$ , the importance of highly relativistic particles in many applications, and the fact that these tracks have the largest number of Čerenkov photons, mean that only the

---

<sup>2</sup>In actual practice, various optical effects may distort ring patterns from ideal circles. The distorted shapes can be computed in particular cases and used as the basis for templates employed by the pattern-recognition algorithm presented below.

dual representations for  $\beta \approx 1$  need be considered in practice.<sup>3</sup> The number of intersections above background in a peak found in the dual space should equal the number of photons detected on the Čerenkov ring which centers on the peak. As will be shown in what follows, peaks or clusters in dual space are a robust indicator of true Čerenkov rings associated with relativistic tracks.

### 3 An Implementation of the Dual-Ring Algorithm

To analyze the efficacy of this “dual-ring” algorithm, we consider a detector image plane divided into cells of equal acceptance  $a$  in vertical and horizontal photon directions  $\theta_V$ ,  $\theta_H$  as indicated in Figure 2. In most practical cases, Čerenkov rings will appear as circles in this space with radii given by

$$\theta_{\check{C}}(\beta) = u(\beta)\theta_0$$

where the limiting-value of the Čerenkov angle for  $\beta \rightarrow 1$  is represented by  $\theta_0$  and the function  $u$ , which describes the relative size of the Čerenkov ring and relative numbers of detected photons. The relative Čerenkov radius  $u$  is related to the particle’s speed and properties of the RICH by

$$u(\beta) = \sqrt{1 - \left[ \frac{(\beta\gamma)_{\text{th}}}{\beta\gamma} \right]^2} = \sqrt{1 - \left( \frac{p_{\text{th}}}{p} \right)^2}$$

where  $p$  is the particle’s momentum,  $\gamma$  is the usual relativistic factor  $1/\sqrt{1-\beta^2}$  and the “threshold” values of  $\beta$  and  $\gamma$  are related to the index of refraction  $n$  of the Čerenkov radiator and the particle mass  $m$  by

$$\beta_{\text{th}} \equiv \frac{1}{n}, \quad \gamma_{\text{th}} = \frac{1}{\sin \theta_0} = \frac{n}{\sqrt{n^2 - 1}}, \quad p_{\text{th}} \equiv m(\beta\gamma)_{\text{th}}$$

The mean number of photons detected on a given ring is  $N_{\text{hit}} = u^2 N_0$ , where the limiting value  $N_0$  depends on the details of the RICH design, particularly the quantum efficiency of the photon detectors and length of the radiator.

---

<sup>3</sup>When the particle’s momentum is considered as a separate degree of freedom, the locus of possible track parameters becomes a surface in a three-dimensional parameter space. Using nomenclature developed in the next section, this surface can be taken as a *sphere* represented by

$$\sin^2 \theta_0 = \sin^2 \theta_{\check{C}} + \left( \frac{m}{np} \right)^2 \quad \text{or} \quad \theta_0^2 \approx \theta_V^2 + \theta_H^2 + \left( \frac{m}{np} \right)^2$$

which has the radius of a  $\beta = 1$  Čerenkov ring and is centered on the detected photon direction coordinates at the point  $m/np = 0$ . One can imagine performing a “dual-sphere” algorithm, similar to the dual-ring algorithm described here, and determine the track direction and relative momentum in a *single* pass. However, the two-dimensional algorithm explored here may prove more efficient for the cases of greatest practical interest, where  $p \gg p_{\text{th}}$ .

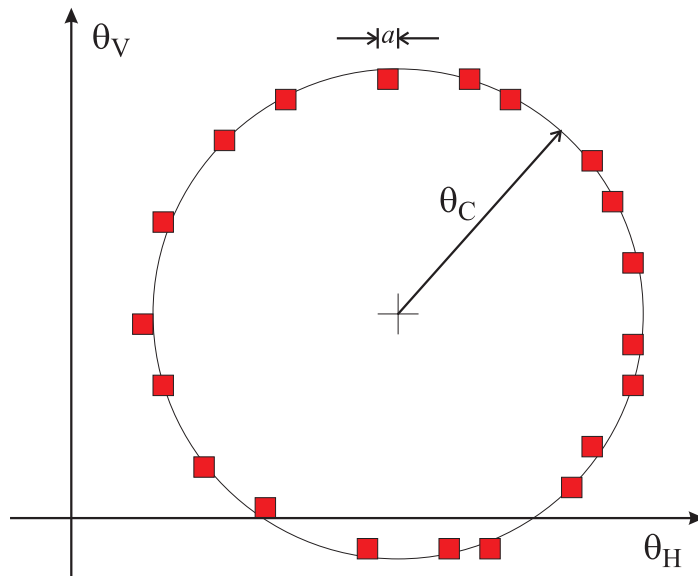


Figure 2: Detector image plane. Detected photons are represented as red squares or cells of size  $a$ .

As an example, the HERA-B experiment [2] employs a RICH detector to tag kaons in a  $CP$ -violation experiment involving  $B$ -particles produced by high energy protons striking a fixed wire target. The HERA-B RICH detects photons with multi-anode photomultipliers having two different cell-sizes,  $a \approx 1.5, 3$  mr, uses  $C_4F_{10}$  gas for the Čerenkov radiator which gives  $\theta_0 = 53$  mr, and is expected to detect  $N_0 \approx 35$  photons per “ $\beta = 1$ ” track. Dispersion in the radiator gas and optical errors are expected to lead to an RMS direction error of  $\sigma_{\check{C}} \approx 0.6$  mr per detected photon.

The simplest implementation of the dual-ring algorithm is to choose a dual space having the same dimensions and cell-size as the detector image plane. Templates can then be constructed for the dual-representations of each photon hit and choice of  $u$ , labeled by  $u_T$ . When the cell size is larger than the RMS spread in Čerenkov angles ( $a > \sigma_{\check{C}}$ ) then unit weights can be assigned to cells lying on the locus of possible track centers and a simple search algorithm can be used to find those cells. We call the set of cells closest to a circle of radius  $u_T\theta_0$  centered on the origin the “dual template.”<sup>4</sup> In the interest of simplicity, the algorithm used in the present analysis finds cells for the dual template by searching in *single* horizontal or vertical steps. This algorithm provides a reasonably uniform cell density over the full dual

<sup>4</sup>We have studied search algorithms where only a single step in either  $\theta_V$  or  $\theta_H$  is taken for finding cells in the dual template and algorithms where diagonal steps  $|\Delta\theta_V| = |\Delta\theta_H| = 1$  are allowed. It is also possible to weight the cells in the dual-representation according to position on the circle. There appear to be different advantages and disadvantages to each of these choices.

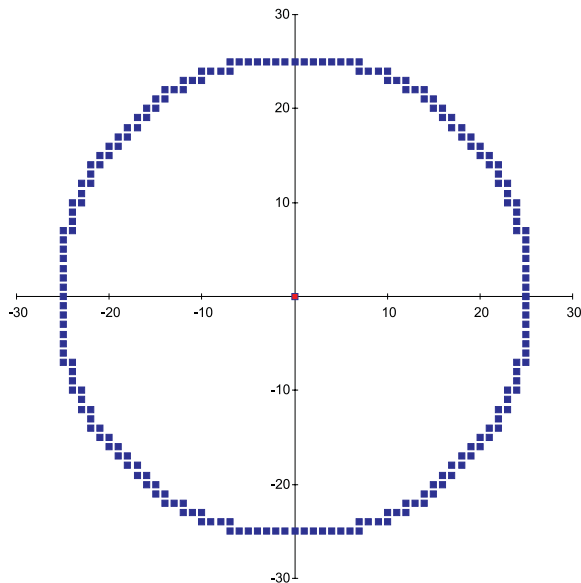


Figure 3: Dual template with a radius corresponding to 25 cells generated by taking single horizontal or vertical steps in sequence to find cells closest to the generating circle.

template, but the total number of cells in the template is somewhat larger than  $2\pi u_T \theta_0 / a$ . A typical dual template having a “radius” of 25 cells is shown in Figure 3.

Once a template is generated for a given  $u_T$ , application of the dual-ring algorithm simply involves incrementing every cell in the dual space lying on a template of some hit by one count for *every* detected photon. If the choice of  $u_T$  matches the actual  $u$  for some set of  $N_{\text{hit}}$  detected photons belonging to a single track, then one of the cells in the dual space—the one corresponding to the track center—will be incremented by  $N_{\text{hit}}$  counts plus possible background from other Čerenkov rings. Cluster-finding techniques can be used to find peaks in the dual space which will correspond to the tracks in the given event with values of  $u$  in the vicinity of  $u_T$ .

The viability of this algorithm depends on the statistical significance of true clusters compared to chance overlaps of dual templates from uncorrelated photon hits. It is clear that this method is most sensitive to tracks with  $\beta \approx 1$  (corresponding to  $u \approx 1$ ) because  $N_{\text{hit}}$  will be largest and the detected photons are furthest away from the peak in dual space corresponding to their track center, which should tend to reduce backgrounds and false clusters, even though the number of template cells being added to the dual space for each photon hit is largest.

To better describe the dual-ring algorithm, we apply it here to a set of four tracks with parameters as given in Table 1. The cell size used is

Track	$p$ (GeV)	$\theta_H$ (mr)	$\theta_V$ (mr)	$u$
muon	10	5	-0.4	0.982
pion	30	-3	12	0.996
pion	12	25	-10	0.975
pion	4	-10	-10	0.747

Table 1: Tracks used in simulation described here.

$a = 2$  mr and the limiting Čerenkov angle is taken to be  $\theta_0 = 52.6$  mr. Photon hits were generated randomly for these tracks assuming the limiting mean number to be  $N_0 = 35$  and the RMS angle error for each photon to be  $\sigma_C = 0.6$  mr.

The pattern of photon hits is shown in Figure 4. A total of 115 photon hits were generated for the four tracks indicated in Table 1. It is not really meaningful to ask which photons are associated with which track. The probability distribution for all tracks is integrated over all cells on the detector image plane. Only then are random numbers chosen to decide which cells are hit. Thus, a given hit cell could be “shared” by more than one track.

Dual spaces for the photon hits shown in Figure 4 were constructed for  $u_T = 0.985$ , which corresponds to the mean velocity of the three highest-speed tracks, and for  $u_T = 0.747$ , which corresponds to the lowest-momentum pion. These are shown in Figures 5 and 6, respectively. Figure 5 shows three sharp peaks, cleanly separated from the background, centered on the  $\theta_V, \theta_H$  coordinates of the parent tracks and having the expected number of counts above background. The low-momentum pion is not visible in this figure. When the dual template is “tuned” for lower speed, as in Figure 6, the high-speed peaks disappear and the low-momentum pion stands well above background, albeit with fewer total counts as expected from the Čerenkov photon yield relationship which scales as  $u^2$ .

## 4 Estimates of Performance

The sharp peaks evident in Figures 5 and 6 clearly indicate the potential of the dual-ring algorithm for finding Čerenkov rings and ring-centers from photon hit information, alone. In this section, we explore analytically the sensitivity of the dual-ring approach.

That a peak should form in the cell corresponding to the true track center with  $N_{\text{hit}}$  counts, on average, when the dual template has a correct value of  $u_T$  is obvious. We want to examine the conditions under which peaks are visible—statistically significant—over the background of dual cell entries from uncorrelated photons or from templates where  $u_T \neq u_{\text{track}} \equiv u$ .

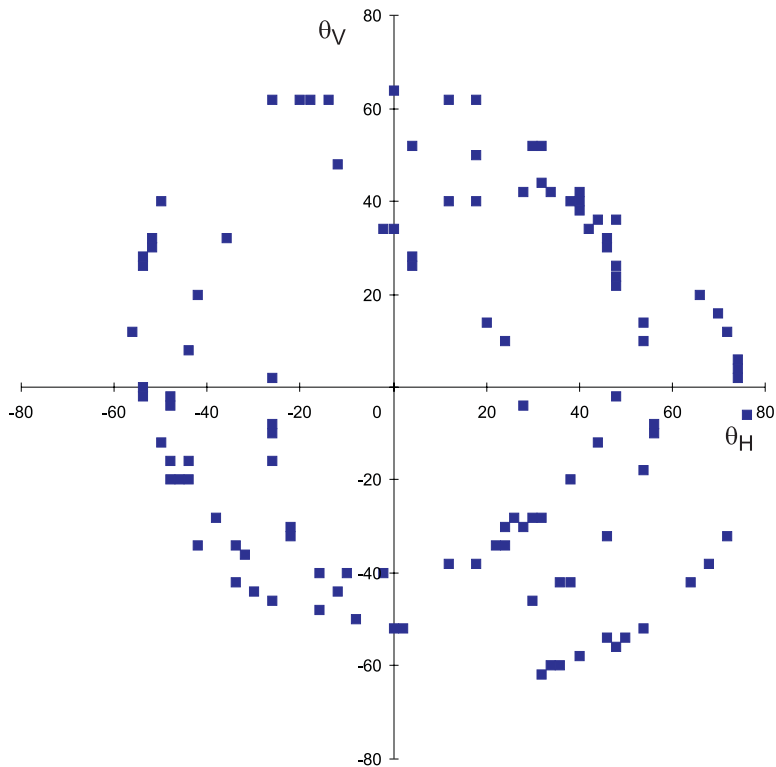


Figure 4: Photon hits generated for the tracks described in Table 1.

A perfect circular template of cells of size  $a$  would contribute  $2\pi u_T \theta_0/a$  counts to the dual space for every photon hit. For the template-generating algorithm used here, “ $2\pi$ ” in this expression should be replaced by a factor around 8. Thus, for every hit, we expect  $8u_T \theta_0/a$  counts to be entered in the dual space. Let  $\omega$  represent the average *occupancy* of detector cells, the fraction hit on a given event. The average occupancy (actually, the mean number of counts per cell) for cells in the dual space will be  $\tilde{\omega} = 8u_T \theta_0 \omega/a$ .

We can define the statistical significance  $\Sigma$  of a peak in one cell of the dual space due to a true Čerenkov ring to be the number of counts above background divided by the mean fluctuations in the background. We assume the background to be: a) smooth, and b) described by Poisson statistics. Under these assumptions, the significance is  $\Sigma = u^2 N_0 / \sqrt{\tilde{\omega}}$ , assuming the correct,  $u_T = u$ , template is used. For various reasons, the cell size adopted for applying the dual-ring algorithm may differ from the actual cell size employed on the detector plane. The observed occupancy will depend on running conditions—track density and background rate—and the choice of cell size. The occupancy will scale like  $\omega = \omega_0 (a/a_0)^2$ , where  $\omega_0$  and  $a_0$  refer to the occupancy and cell size on a “reference” detector plane. Including this factor allows us to make parametric studies of the statistical significance

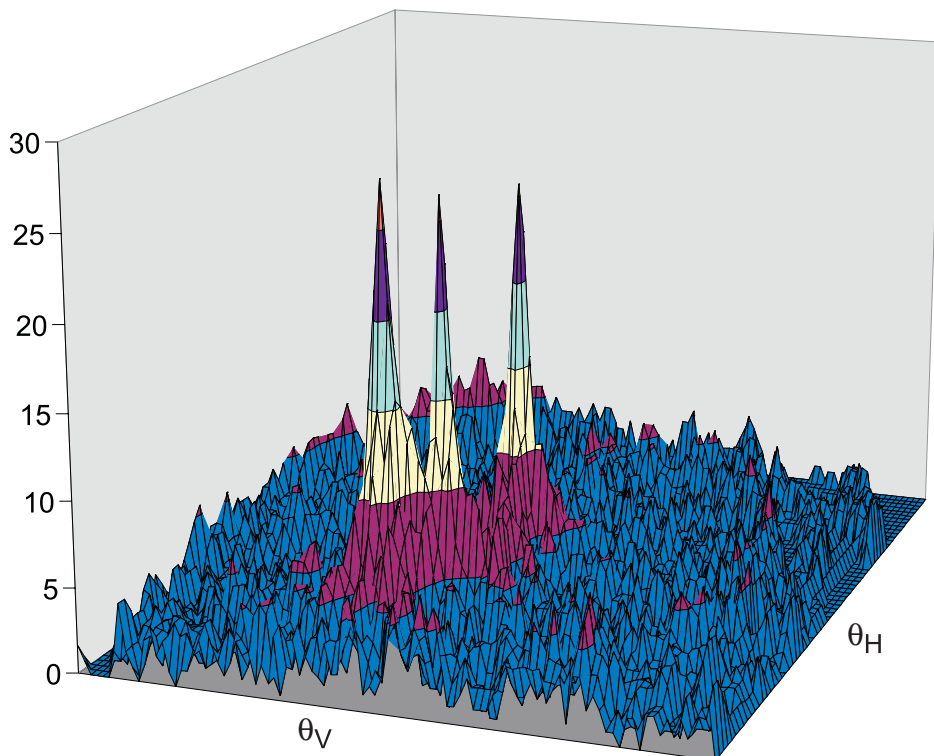


Figure 5: Dual space for the photon hits shown in Figure 4 with the parameter,  $u_T = 0.985$ . The number of counts per cell is plotted versus the  $\theta_V, \theta_H$  coordinate of the cell.

$\Sigma$  under *fixed* running conditions according to:

$$\Sigma = \frac{N_0}{\sqrt{8\theta_0\omega_0/a_0}} u^{3/2} \left(\frac{a_0}{a}\right)^{1/2}$$

Cluster-finding techniques may be the best way to identify peaks in dual space, in which case blocks of several contiguous cells may be searched for a signal. The statistical significance of peaks found in blocks of cells will be essentially the same as that derived above because the signal will scale *linearly* with block size, while background scales as the *area* of the block of cells. The significance, as defined here, is the ratio of the signal to square-root of background and, thus, is *invariant* to cluster size to a first approximation. Should there be more than one track-center present in a given cluster, the number of signal counts will give a clear indication of the overlap.

For the parameters used in this note,  $\Sigma \approx 25u^{3/2}\omega(\%)^{-1/2}$ , where the detector-plane occupancy  $\omega$  is expressed in % and the cell size used for the algorithm is assumed to be the same as that of the reference detector. To ensure good efficiency for detecting real tracks and low probability for

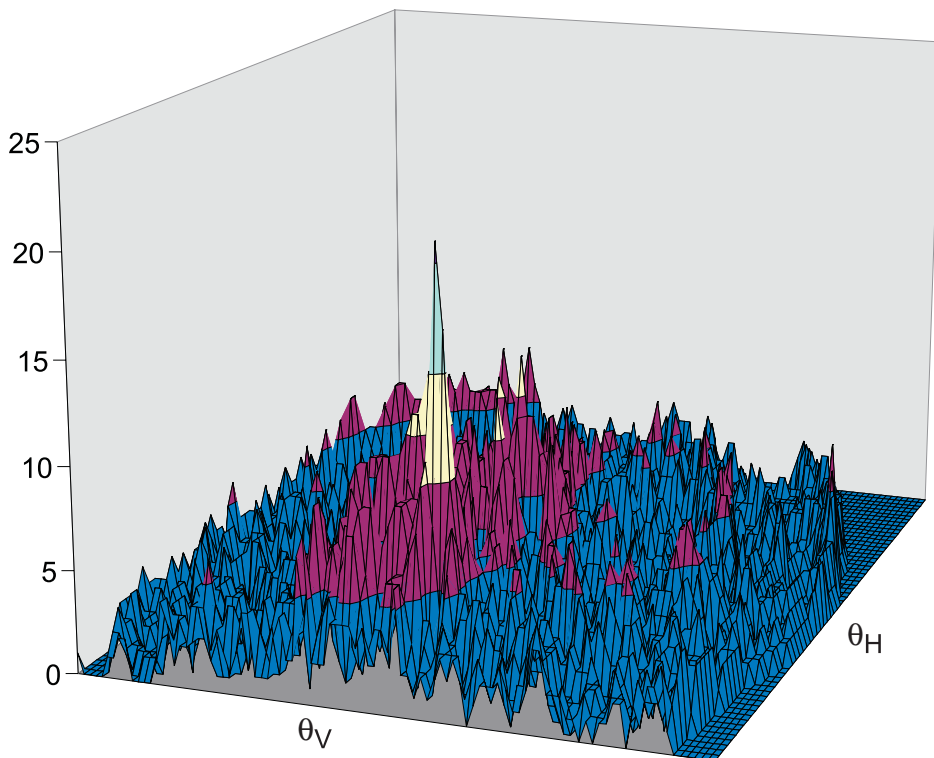


Figure 6: Dual space for the photon hits shown in Figure 4 with the parameter,  $u_T = 0.747$ . The number of counts per cell is plotted versus the  $\theta_V, \theta_H$  coordinate of the cell.

creating false tracks, we probably want to require  $\Sigma \gtrsim 8$ . This should be possible for high-speed tracks ( $u \approx 1$ ) as long as the occupancy is limited to roughly  $\omega \lesssim 10\%$ . If the occupancy is less than 1% for the parameters used here, it may be possible to identify track centers at the  $8\text{-}\sigma$  level for velocity parameters as low as  $u \gtrsim 1/2$ , which corresponds to momenta  $p \gtrsim 1.2p_{\text{th}}$ .

If the relative radius  $u_T$  of the dual template does not exactly match the actual track parameter  $u$ , a circle of radius  $\theta_0|u - u_T|$  forms around the actual track center by the overlapping templates. We can estimate the number of counts  $n_{\text{ovl}}$  in cells forming this “overlap” circle by calculating the fraction of cells on a given dual template which are within one cell dimension of the overlap circle. The result is

$$n_{\text{ovl}} = \frac{\sqrt{2}}{\pi} N_{\text{hit}} \sqrt{\frac{u_T a}{u|u - u_T|\theta_0}}$$

This expression exhibits a somewhat slower fall-off with distance from the actual track center than the case for correctly tuned templates ( $\sim 1/r$ ), but indicates that by the time the radius assumed in the dual template

differs from the true Čerenkov radius by more than a few cell dimensions, the number of entries in overlap circles will drop to the background level, or, at least, to well below the signal level. For dual templates close to the correct radius ( $|u - u_T|\theta_0 \sim a$ ), a cluster that includes the overlap circle will have about the same statistical significance as the true peak, as discussed previously.

The emergence of peaks in dual space as  $u_T$  is tuned was studied by an explicit calculation of the algorithm for a single 6 GeV/ $c$  pion ( $u = 0.896$ ) using the parameters described previously. The cell size  $a$  and limiting Čerenkov angle  $\theta_0$  imply a “step size” in  $u_T$  of approximately 0.04 units. Figure 7 shows the dual space for this situation where  $u_T$  was varied over the range  $0.80 \leq u_T \leq 1$  in steps of 0.04; the central value, 0.90, was also computed. The figure shows the emergence of a clear peak from a “crater”<sup>5</sup> and back again when  $u_T$  is varied by only  $5a/\theta_0$ . Indeed, the central three templates, where the radius is incremented by about 1/2 cell between templates, show significant changes in the shape of the peak, clearly indicating the correct value of  $u$  to be slightly below 0.90. The craters that form when  $u_T$  is de-tuned, even by as few as two cells, have the characteristics estimated above.

We conclude that the resolution of the dual-ring algorithm for determining the relative Čerenkov ring radius is

$$\delta u \lesssim \frac{a}{\theta_0}$$

Offline data analysis techniques, such as likelihood fits and/or cluster analyses, that make use of patterns found by the present algorithm or other means, should be able to reduce the error in determining  $u$ , as well as uncertainties in track directions, below the single-cell levels described here.

## 5 Areas for Further Work

The two main lines of work needed to pursue the dual-ring algorithm for pattern recognition in RICH systems are 1) to further refine and explore the algorithm, and 2) to develop computer codes and possible hardware processors that can carry out the algorithm rapidly.

Some of the issues that can be studied with more sophisticated monte carlo simulations include the effects of nearby tracks and possible pathological backgrounds that might arise under more realistic models of detector performance and experimental conditions.

The algorithm might be improved by using non-integer cell-weights or even likelihood weighting. Cell-weighting should improve the signal/noise

---

<sup>5</sup>The number of counts at the center of the dual space actually goes to zero in this calculation at the “bottom” of the crater.

ratio, significance of peaks and determination of track directions and speed. More work is needed on the actual peak-finding. Again, these points can be addressed using standard monte carlo techniques.

Trigger-processors based on the dual-ring approach would seem attractive for many high-rate experiments that can or must make use of Čerenkov detector information. Such processors could provide both tracking and particle identification information. The dual-ring algorithm offers the potential of very rapid and accurate determination of high-speed track parameters, but presents serious challenges to hardware (and software) designers because of the large number of “connections” between the detector image plane and the track center dual space. In principle, the algorithm is a very simple one-to-many, many-to-one cross-bar switch *for each desired value* of  $u_T$ . The problem is that “many” can easily mean over 100 connections per cell between two arrays of several thousand cells each. A related problem is the software implementation needed to reduce the number of computation steps so that practical analysis codes can be developed which will not significantly impede event reconstruction.

## 6 Conclusions

We have described a simple and powerful algorithm for finding Čerenkov rings amongst other rings and backgrounds that uses only the photon hit information supplied by the RICH detector. Assuming detector performance characteristics well within today’s state-of-art, the statistical power of the method should permit efficient detection of high-speed tracks in moderately noisy environments with relatively few false tracks.

## References

- [1] *Experimental Techniques of Cherenkov Light Imaging*, edited by E. Nappi and T. Ypsilantis, Nucl. Instr. Methods **A 343** (1994).
- [2] HERA-B *Technical Design Report*, DESY Report **DESY-PRC-95/01**, January, 1995.

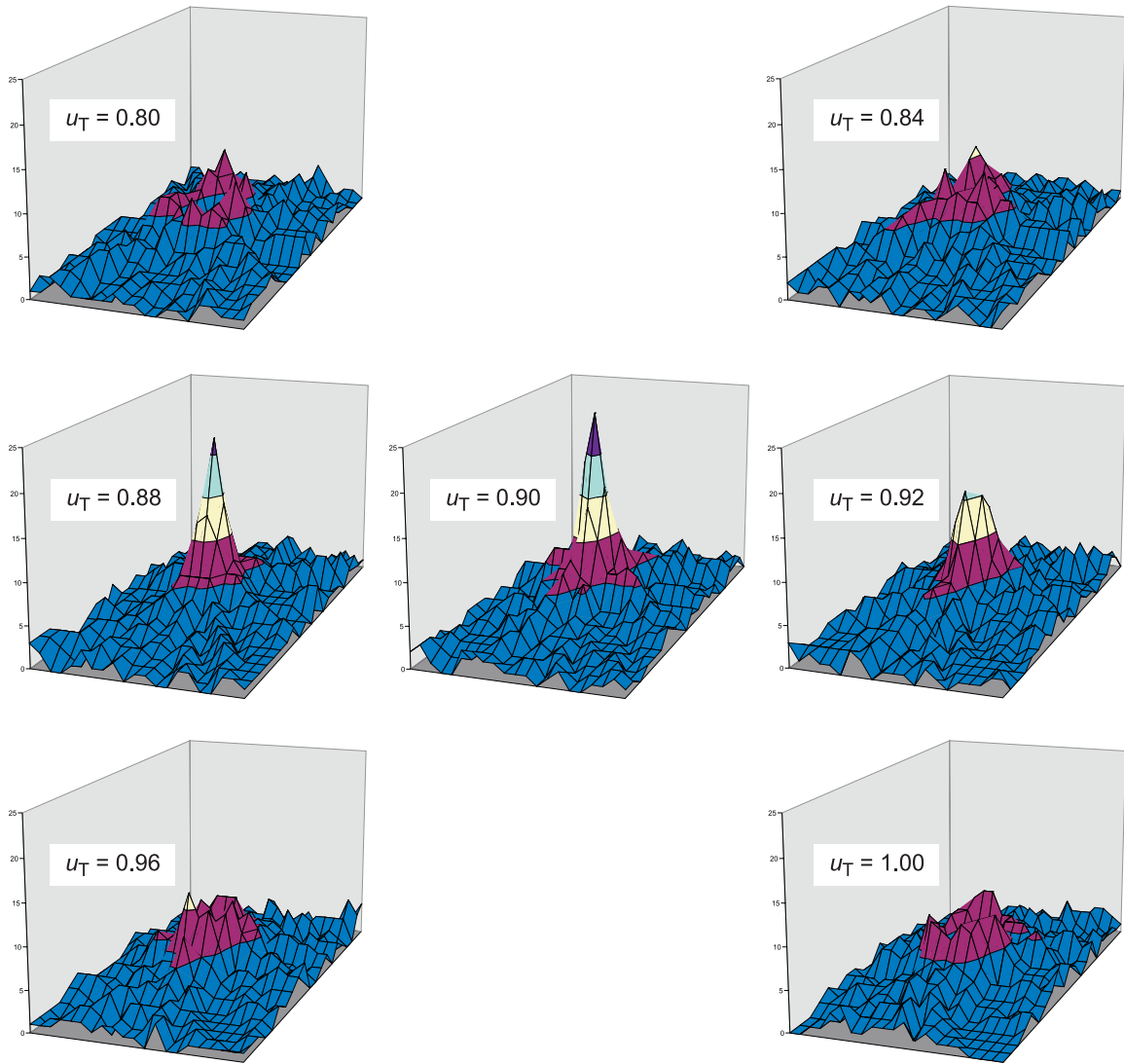


Figure 7: Dual space for a single  $u = 0.896$  track computed with different dual templates having the values of  $u_T$  indicated.